*Salim Çalışkan**

INVESTIGATION OF FAILURE ANALYSIS FOR AISI 4340 STEELS ON NEAR THRESHOLD REGION

ISTRAŽIVANJE I ANALIZA LOMA AISI 4340 ČELIKA U OBLASTI BLIZU PRAGA ZAMORA

Originalni naučni rad / Original scientific paper
Rad primljen / Paper received: 6.03.2024
https://doi.org/10.69644/ivk-2025-03-0413

Adresa autora / Author's address:
Turkish Aerospace Inc., Ankara, Turkey
S. Çalışkan https://orcid.org/0000-0002-9276-8492
*email: salim.caliskan@tai.com.tr

Keywords
- failure analysis
- fatigue
- heat treatment
- steel
- threshold

Abstract

Fractography investigations may unveil the pathway behind the failure by examining the fracture surfaces, and it is a subject that requires careful consideration, particularly in aircraft structures. Fractography can identify crack initiation sites, the direction of crack growth, any associated defect in the microstructure, the environmental effect on fracture, and the type of stress within the material. Proper investigations are needed to identify the origin of failure, the direction of crack propagation, and the related fracture mechanism. This is achieved by assessing the marks on the fracture surface under the microscope. Most of the failures are the result of multiple influences and are rarely single in metallic alloys. Fatigue striations are the most prevalent indicator on the fractured surface of ductile metal alloys in the Paris region of the crack growth curve. In this study, failure analysis is performed after performing crack growth tests for different microstructures in AISI 4340 steels, especially in the near threshold region, and root causes of failure are compared for each case. Crack propagation and morphological changes up to fracture have been observed in AISI 4340 steel. Under SEM and stereomicroscope examination, each stage of crack propagation is detailed with failure analysis.

Ključne reči
- analiza loma
- zamor
- termička obrada
- čelik
- prag zamora

Izvod

Fraktografska istraživanja mogu otkriti put ka lomu ispitivanjem površina preloma, a to je tema koja zahteva pažljivo razmatranje, posebno kod konstrukcija letelica. Fraktografijom se otkrivaju mesta inicijacije prslina, pravci rasta prslina, sve asocirane greške mikrostrukture, uticaji okoline na lom, kao i tipovi napona u materijalu. Potrebna su pogodna istraživanja radi otkrivanja uzroka loma, pravca širenja prsline, kao i odgovarajućeg mehanizma loma. Ovo se postiže ocenjivanjem tragova na površini loma pod mikroskopom. Većina lomova nastaju kao rezultat višestrukih uticaja i retko su pojedinačni uticaji kod legura metala. Linije zamaranja su najčešći indikator na prelomnoj površini duktilnih legura metala u Parisovoj oblasti krive rasta prsline. U ovom radu se analiza loma izvodi posle ispitivanja rasta prsline kod različitih mikrostruktura čelika AISI 4340, posebno u oblasti blizu praga zamora, a zatim se uzroci loma upoređuju za svaki dati slučaj. Širenje prsline i promene u morfologiji sve do pojave loma su uočene kod čelika AISI 4340. Korišćenjem SEM i stereomikroskopskih ispitivanja se svaka faza u razvoju prsline se detaljno istražuje analizom loma.

INTRODUCTION

Over the past half a century, there have been many breakthroughs in identifying fatigue crack growth mechanisms. During this period, failure analysis specialists have advanced with numeric and computational methods that can handle cracks of almost any size and shape in any sort of material. The involvement of TEM and SEM, and the development of testing machines have greatly enhanced our comprehension of the standards controlling fatigue crack initiation and propagation /1/. Fracture investigation explicates the mechanism behind fracture by observing the fracture surface. As a matter of course, fracture surface analysis can identify crack initiation locations, crack propagation directions, associated microstructural defects, environmental influences on fracture, and types of stresses experienced by the material. The main object of failure analysis is to recognise the fundamental reason causing the failure. No matter what material type, it may be due to one of the successive reasons: manufacturing process, specimen geometry, material properties or operating conditions. A combination of aforementioned causes can lead to cataphoric failure. For instance, increased stress concentration because of the geometry or improper material selection can lead to premature failure. Analysis methods have advanced to the point that inconceivable extensive post-failure investigation has become a standard technique in fractography, /2/. Significant examinations are required to identify the cause of failure, evaluate the path of crack propagation, and identify the related failure mechanism. The indicated is achieved by fundamentally examining the clues present on the failure surface. Nearly all failures have multiple causes and rarely occur in isolation. A typical fatigue fracture exhibits striation, beach marks, and ratchet marks on the fracture surface of the metal material, facilitating investigation of crack initiation and crack growth direction /3/.

Fracture surface analysis is important for evaluating fatigue crack propagation and revealing the mechanisms behind fracture. For the purpose of illustration, brittle failures lead to very little material deformation across the failure area. In contrast, ductile fractures can induce impressive deformation. The growth of intragranular cracks is highly planar and exhibits crystallographic behaviour with fracture facets associated with displacements along the close-packed planes of many low-stacking-fault-energy superalloys. This can be clearly observed, especially in the region of the threshold region, upon the size of the cyclic plastic zone that converges on the average grain size /4/. The amount of ductility seen in the failure surface is an important point of the stress or environmental impact to which the specimen has been exposed under stress. Specifically, higher stress leads to greater roughness and ductility. On the contrary, lower stress usually leads to lower ductility and lower fracture surface roughness. Lower stresses and brittle fractures are closely related to smoother fracture surfaces. Such surfaces may also happen as a result of severe environmental stress cracking. Fractures with slow crack propagation under cyclic loads can also produce highly smooth fracture surfaces. At higher loads, the fracture surface usually becomes more and more rough /5/. The fatigue crack surface noticeable to the naked eye exhibits a nearly planar fracture surface, which is exhibitive of fatigue. Ultimately, it flowed perpendicular to the direction of the applied load. Shear lip stretches as the crack growth rate increases near the unstable crack growth region. When the shear lip completely covers the cross-sectional area of the specimen, catastrophic failure usually occurs in the form of shear cracks, /6/.

Revealing post-failure clues and selecting appropriate components for SEM inspection are one of the first processes in fractography. Additional considerations to consider include site surveys, failure history, material quality, maintenance and substitution documentation evaluations, and historical failure rates for specific items. Analysis begins with a visual inspection of the failure region of the part with the naked eye prior to microscopy. Optical microscopy helps characterise fracture surfaces, identify crack areas and fracture mechanisms, and reveal microstructural flaws that cause cracks. In detail, SEM can help identify rupture and identify the origin of crack initiation by self-evident marks /7/. As a standard, an ultrasonic bath is utilised to sterile the failure surface. The samples are then examined by SEM and then measurements are generally performed in the plane strain regime because the properties near the edge can change significantly under plane stress. Low magnification images are taken at different crack lengths to show the progress of the crack propagation test.

Striations on the fracture surface can be caused by various conditions such as fatigue, slow crack growth, and rapid brittle fracture. These successive lines are isolated by the fracture region and can be related to crack arrest and crack growth under alternating loads. A biaxial stress state arises at the outer part of the crack tip due to the disappearance of the stress elements normal to the free surface. The distribution of striations on the fracture surface is related to the exposed stress ratio. Hence, striations are expected to reduce as the stress ratio increases /8/. Fatigue striations are the foremost accepted manifestation of strain marks on fracture surfaces of ductile metal alloys in the steady-state crack growth rate region. The Laird model is one of the best-known models for the striation mechanisms /9/. Laird viewed the striation as a continuous form of crack tip blunting and re-sharpening accompanied by steady crack growth. Since the Laird model is practically applicable, the striation spacing is readily used as a crack propagation rate estimation principle. Nevertheless, the striation may not be used to validate a direct proportional relationship between fatigue striation intervals and fatigue crack growth rates /10/.

Inclusive investigation of fracture surfaces makes easier the identification of several fatigue fracture properties. Ratchet traces show the consequences of various fatigue crack initiation causes due to high stress concentrations, and beach marks show fatigue crack growth and distinctly show changes in crack growth rate. Secondary cracks can be explained due to high non-uniform stresses during catastrophic failure. It is critical to note that the presence of ratchet marks is presently related to fatigue phenomenon. Ratchet marks look like small cracks that form and grow in the plane under maximum shear stress. Evidence of fatigue failure can be investigated in SEM evaluation by examining fatigue striations, secondary cracks and ratchet marks /11/. Under high stress loading, the fatigue crack propagation rate increases significantly, leading to irregular fatigue striations /12/. Li et al. explained this phenomenon in their study because pitting corrosion occurs when the stress intensity load is high /13/. It can be seen that the number of pits increases as the crack propagates, and that pitting is increasingly the dominant failure mechanism at high crack growth rate compared to striations. When the threshold range is reached, crack propagation is affiliated with blunting and re-sharpening process. In contrast, the formation of fatigue striations is driven by the interaction between crack tips and slip bands as described in the dislocation-based model /14/. Large stress intensity loads increase the stress in front of the crack tip, leading to the formation of microcracks with deformation. Dislocations unloosed from cracks can also increase plastic strain under fatigue loading, causing micro void expansion and coalescence.

MATERIALS AND METHODS

Fracture surface analysis aimed to investigate microstructural features after fatigue failure through crack growth specimens. Two different microstructures are studied on AISI 4340 steels via heat treatment. The chemical composition of the steel is presented in Table 1. Specimen configuration is chosen as the single edge bending (SEB) type for the following reasons: the extended geometry provides additional working space when performing crack growth tests. Relatively less force is required for the same stress value compared to other sample configurations. Grip feature is not required when assembling specimens for the test setup interface since gripping force directly affects compliance results. The specimen geometry is 12 mm thick, 24 mm wide and 110 mm long, compatible with plain strain assumptions with fracture mechanics in accordance with ASTM E647-23

/15/. Additionally, an artificial 8 mm notch in the centre of the specimen is formed by EDM to enable sharp stress concentration.

Table 1. Chemical composition of the material (wt.%).

Alloy	Fe	C	Ni	Cr	Mn	Mo	P	S	other
AISI 4340	96.2	0.38	1.65	0.7	0.65	0.2	0.01	0.01	0.2

After machining, specimens are heat treated as a final process to comply with AMS 2759/1D /16/. Subsequently, annealed and tempered microstructures are separately obtained at different furnace temperatures and cooling rates. Accordingly, the previous one is heated at 840 °C for 1 hour after furnace stabilisation, followed by air cooling to achieve the final microstructure. The latter is heated at 810 °C for 1 hour, then oil quenched, and finally furnace tempered at 600 °C for 3 hours followed by air cooling.

A total of 12 specimens are studied for crack growth tests. After heat treatment, the following mechanical properties are determined for each specimen type. Tempered specimens have an ultimate strength of 1080 MPa and a hardness of 29 HRC, while the annealed specimens have an ultimate strength of 820 MPa and hardness of 17 HRC. In terms of microstructure, tempered microstructure results in tempered martensite with stable ferrite and cementite phases; on the other hand, annealed microstructure shows pro-eutectoid ferrite phase and pearlite phase as seen in Fig. 1.

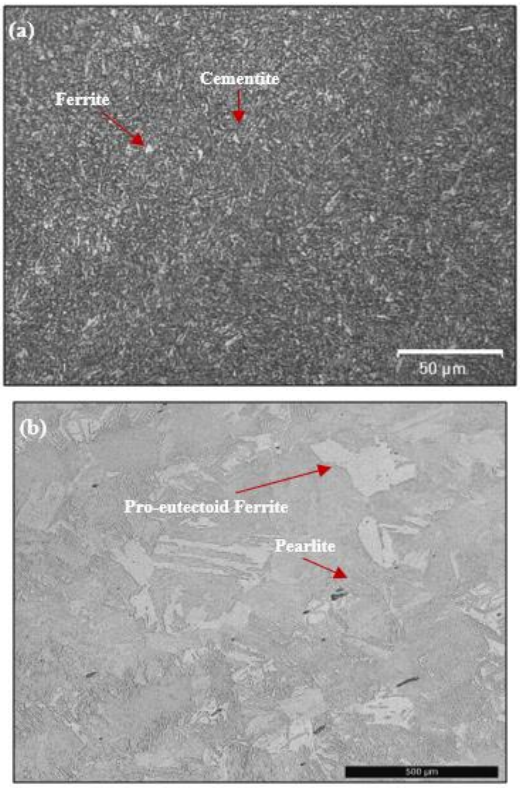

Fig. 1 Optical micrographs of the specimens: tempered (a) and annealed condition (b)

Crack growth tests are performed at room temperature (23±2 °C) and normal humidity conditions in accordance with ASTM E647-23. Test specimens are inserted on RUMUL brand CRACKTRONIC test bench and loaded at predefined stress ratios at the resonance test frequency, the first rigid body mode of the entire system. On the other hand, failure analysis is carried out on a ZEISS brand SEM device at TAI's premises.

CRACK GROWTH TESTS

Crack growth tests are performed under three different stress ratios: two specimens of each case are tested with R of -1, 0.1 and 0.7 for each microstructure. In summary 12 specimens are loaded to determine the threshold values of AISI 4340 steel and followed by fracture surface analysis. To minimise the effects of the load history, a pre-crack test is carried out for each specimen in a four-point bending test setup under compressive loading. Eventually, the precracking test created natural pre-crack ahead of the artificial notch by ensuring a crack length longer than the length of the three monotonic zones formed after initial compressive loading. The purpose of this test is to obtain an accurate threshold after performing a crack growth test. After natural crack is formed, specimen is ready to begin crack growth test, the first step of which is the crack stabilisation test under constant amplitude loading. The tricky part is to estimate initial ΔK value. If the value is insufficient, crack growth rate will start to decrease although ΔK increase. In this case, ΔK can be increased by 10 % increments. If the stress is high enough, the crack growth rate starts to increase after overcoming closure effects and crack size advances. In this stage, crack stabilisation should be achieved after the crack has propagated 1-2 mm to eliminate residual stress effects. After crack stabilisation, load reduction is done under constant ΔK. The crack growth rate is very slow on near threshold region, indicating that the crack is not propagating. In this study, the crack growth rate criterion is taken as 10^{-10} m/cycle to ensure that threshold is reached and corresponding stress intensity value is used as the threshold stress. Figure 2 exhibits threshold results obtained after performing crack propagation tests. The corresponding threshold value is determined by averaging the two-test data for each case. Eventually, variation in threshold with stress ratio can be estimated within a predefined stress ratio range. R of 0.7 is accepted as stress ratio at which no closure effects are observed near the threshold. When the threshold data are normalised with closure free data, the threshold values converge to each other for each microstructure.

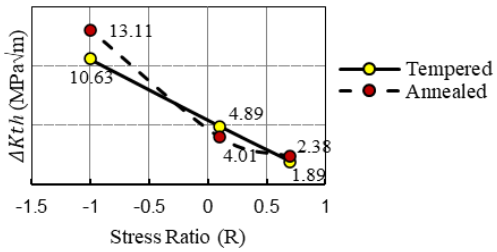

Figure 2. Threshold values for each microstructure with varying stress ratio.

FAILURE ANALYSIS

After reaching the threshold region and completing load reduction test, all the specimens are broken under constant amplitude loading for failure analysis. The specimens are then stored in silica bags to prevent corrosion prior to SEM

analysis. Inclusive observation of fracture surface provides to examine the root cause of fracture mechanics. In this study, the fracture surface is observed using a stereo microscope and SEM. They envision examining each phase of the crack growth test based on the colour contrast: pre-cracking, crack stabilisation, load reduction and fast fracture zone. Figures 3 to 7 explicitly show how cracks initiate and propagate during crack growth tests for each microstructure.

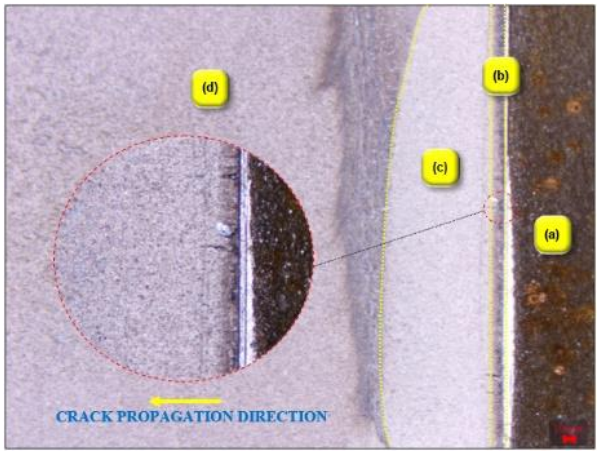

Figure 3. Macro fractography showing fracture surface on stereo microscope: a) notch region; b) compression-compression precracking region; c) crack stabilisation region; d) load reduction region.

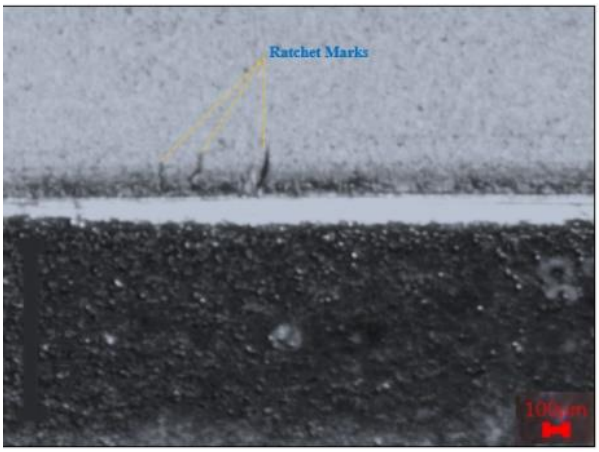

Figure 4. Multiple crack initiation sites observed on compression-compression precracking stage because of severe loading.

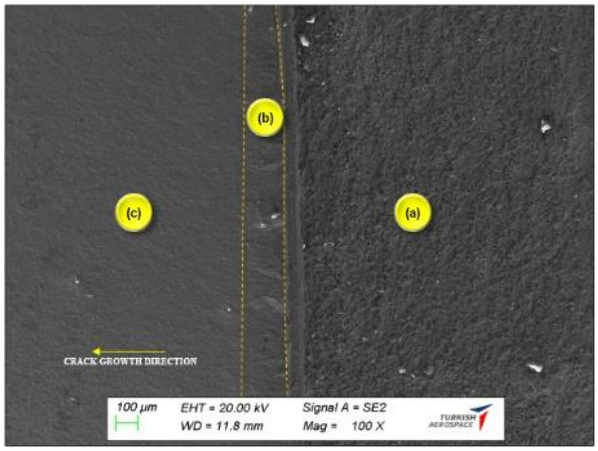

Figure 5. Micro fractography under SEM, regions: a) notch; b) compression-compression precracking; c) crack stabilisation.

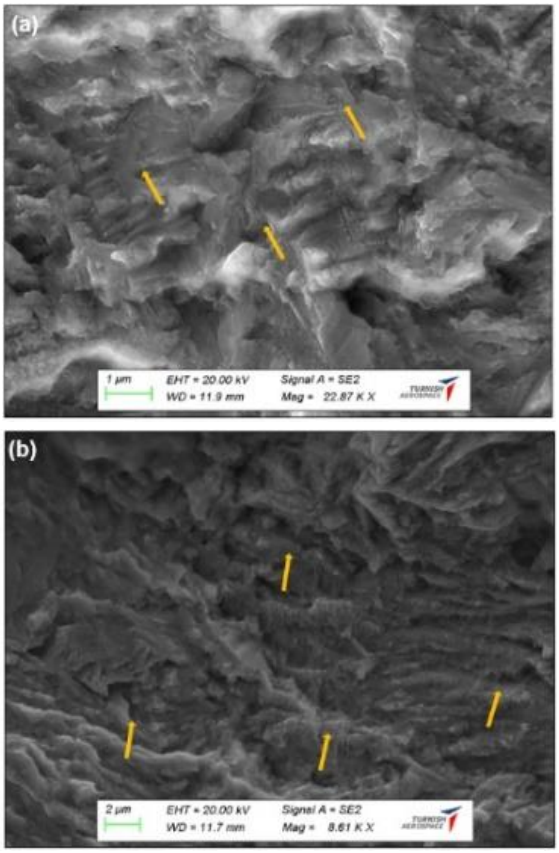

Figure 6. Fatigue striations on: a) tempered; and b) annealed specimens, (arrows show local crack growth direction).

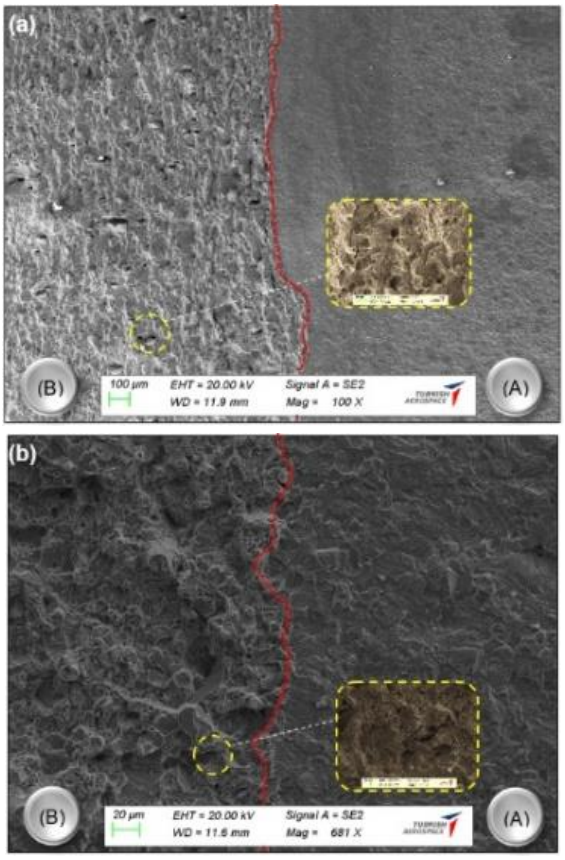

Figure 7. Transition from crack growth (A) to fast fracture region (B) for: a) tempered; and b) annealed specimens.

DISCUSSION

Mechanical characteristics of material and microstructural features directly influence fatigue crack propagation rate near threshold based on persuasive studies. Fatigue failure behind of steel is mainly induced by the striation mechanism, and microstructure and stress ratio play less role in the stable growth part of the crack growth curve. As stress approaches the threshold stress, the crack propagation rate is extremely vulnerable to both load ratio and microstructure, as a result the transitions of striation grow to static failure modes such as cleavage and intergranular failure. Microstructure and load ratio not only have a relatively large effect on the crack propagation rate at low stress intensities near the threshold but are also highly sensitive to crack closure and environmental influences. Materials with a ferrite-pearlite structure exhibit greater roughness in case of applied less stresses than those with a martensite structure. The ferrite phase exhibits striation pathways, in contrast to the pearlite phase, which did not exhibit striations. Another mechanism is entailed in martensitic materials. Relatively less striations are visible, however, fine secondary cracks are visible near the threshold region, while harsh cracks appear at high stress levels. The pearlite phase is tougher than the ferrite phase and plainly confines the deformation of ferrite in the plastic region throughout crack growth. Plastic deformation makes the pearlite structure unable to preserve its strength after repeated hardening, and the strength and plastic deformation are disbursed to adjacent ferrite zones. Through each loading step, this pointed increase in strain causes the growth of microcracks in the ferrite colony, ultimately leading to the fracture of the ferrite colony. An apparently anomalous 'bounce effect' is monitored in the annealed microstructure with ΔK around 13.1 MPa$\sqrt{m}$ and R of -1 stress ratio. To rephrase it, the crack growth rate first decreases as ΔK decreases and then increases as ΔK decreases. This could be a sign that the remote closure has been removed. The earliest drop in crack growth rate can lead to crack retardation because of remote plasticity-induced crack closure. Then, as the crack growth test continues, the surface of the crack breaks with remote closure effect and finally leading to a reduction of the remote closure effect to the crack tip. The severe surface roughness of the pearlite-ferrite structure compared to the martensite structure is a different parameter that affects the crack propagation mechanism. In the pearlite-ferrite structure, striations are dominant in the crack propagation period. However, instead of striations, multiple secondary microcracks are present on the fracture surface of the martensitic microstructure. The threshold value for the annealed material is significantly higher than the material having martensitic phase. On precracking stage, multiple cracks are observed due to severe compressive-compressive loading under SEM investigations. Fast fracture zone is the quasi-cleavage for tempered specimens and the cleavage morphology for annealed specimens. The observable number of dimples is highest in the tempered fast fracture zone than in the annealed fast fracture zone. Dimple elongation was not discovered due to axial loading, and no shear component is available at fracture, i.e., this indicates that fast fracture occurred under axial loading.

CONCLUSIONS

Microstructural characteristics have an important place in the area of fracture mechanics and failure analysis investigation, enabling examination of microstructural characteristics. The fatigue crack growth phenomenon is confined to a small region ahead of the crack tip and revealing the root cause of the mechanism behind failure can be valuable by using available tools. Microstructural dissimilarity in any metals is frequently ascribed to the heat treatment method during production and can influence mechanical properties like yield strength and hardness, causing differences in the size of plastic zones. This affects fatigue crack propagation characteristics and can lead to different threshold data. The following conclusions can be reached from this study.

- All specimens of each microstructure show the same appearance in terms of fracture surface appearance and the mechanism behind failure, which is indicative of the precision of the dataset.
- Although failed specimens were stored in silica bags and degreased and dried to eliminate any stain, some of the fracture surfaces were contaminated, so analysis of these areas was omitted.
- Crack initiation is caused by surface discontinuities that act as stress concentrators in creation of natural crack.
- Ratchet marks are clearly visible on fracture surface, and multiple cracks are likely to occur due to sharp stress concentration.
- Secondary cracks are observed in both microstructures because of the high stress concentration during the precracking stage of crack growth test.
- Fast fracture zone exhibits fully ductile character in both microstructures and dimples are clearly seen in tempered specimens compared to the annealed ones.
- The near-threshold fracture surface analysis of tempered specimens conformed of flat and ductile transgranular modes with a discrete portion of intergranular separation because of tempered martensite embrittlement; on the other hand, the fracture of annealed specimens is very planar and transgranular.
- Near threshold stress values are inversely proportional to increasing stress ratio. Annealed specimens typically exhibit higher threshold.

ACKNOWLEDGEMENTS

Authors acknowledge Turkish Aerospace Inc.

REFERENCES

1. Sunder, R. (1995), *Studies on fatigue crack growth for airframe structural integrity applications*, Sadhana, 20(1): 247-285. doi: 10.1007/BF02747293
2. Peel, C.J., Forsyth, P.J.E. (1908), *The analysis of fatigue failures*, In: Int. Proc. Council of the Aeronautical Sciences, 12th Congress, Munich, West Germany, 1980, New York, American Inst. of Aeronautics and Astronautics, Inc., ICAS-80-0.3, 1980, pp.18-29.
3. Parrington, R.J. (2003), *Fractographic features in metals and plastics*, Adv. Mater. Processes, 161(8): 37-41.
4. Gao, Y., Ritchie, R.O., Kumar, M., Nalla, R.K. (2005), *High-cycle fatigue of nickel-based superalloy ME3 at ambient and elevated temperatures: role of grain-boundary engineering*, Metall.

Mater. Trans. A, 36(12): 3325-3333. doi: 10.1007/s11661-005-0007-5
5. Hayes, M.D., Edwards, D.B., Shah, A.R., Fractography in Failure Analysis of Polymers, 2nd Ed., William Andrew, 2024. ISBN 9780443291494
6. Schijve, J. (1999), *The significance of fractography for investigations of fatigue crack growth under variable-amplitude loading*, Fatigue Fract. Eng. Mater. Struct. 22: 87-99. doi: 10.1046/j.1460-2695.1999.00147.x, 1998.
7. Zamanzadeh, M., Larkin, E., Mirshams, R. (2015), *Fatigue failure analysis case studies*, J Fail. Anal. Preven. 15(6): 803-809. doi: 10.1007/s11668-015-0044-3
8. Ranganathan, N., Sedghi, N., Joly, D., et al. (2012), *A method for quantitative fatigue fracture surface analysis*, In: Proc. 4th Int. Conf. on Crack Path, 2012, Gaeta, Italy. hal-01689617. https://hal.science/hal-01689617v1
9. Laird, C., Chapter: The Influence of Metallurgical Structure on the Mechanisms of Fatigue Crack Propagation, In: J.C. Grosskreutz, STP415-EB Fatigue Crack Propagation, ASTM Int., 1967. doi: 10.1520/STP47230S
10. Xue, Y., El Kadiri, H., Horstemeyer, M.F., et al. (2007), *Micromechanisms of multistage fatigue crack growth in a high-strength aluminum alloy*, Acta Materialia, 55(6): 1975-1984. doi: 10.1016/j.actamat.2006.11.009
11. Miranda, R.S., Cruz, C., Cheung, N., Cunha, A.P.A. (2021), *Fatigue failure analysis of a speed reduction shaft*, Metals, 11 (6): 856. doi: 10.3390/met11060856
12. Meyers, M.A., Chawla, K.K., Mechanical Behavior of Materials, 3rd Ed., Cambridge University Press, 2025. ISBN 9781108 837903
13. Li, H.F., Zhang, P., Zhang, Z.F. (2022), *A new fatigue crack growth mechanism of high-strength steels*, Mater. Sci. Eng.: A, 840: 142969. doi: 10.1016/j.msea.2022.142969
14. Neumann, P. (1969), *Coarse slip model of fatigue*, Acta Metallurgica, 17(9): 1219-1225. doi: 10.1016/0001-6160(69)90099-6
15. ASTM E647-15e1, Standard Test Method for Measurement of Fatigue Crack Growth Rates, ASTM Int., West Conshohocken, PA, 2015.
16. SAE Standard AMS2759/1D, Heat Treatment of Carbon and Low-Alloy Steel Parts Minimum Tensile Strength Below 220 ksi (1517 MPa), SAE Int., 2007. doi: 10.4271/AMS2759/1D